

Article

Unraveling the Synthesis of $\text{SbCl}(\text{C}_3\text{N}_6\text{H}_4)$: A Metal-Melaminates Obtained through Deprotonation of Melamine with Antimony(III)Chloride

Elaheh Bayat , Markus Ströbele and Hans-Jürgen Meyer *

Section for Solid State and Theoretical Inorganic Chemistry, Institute of Inorganic Chemistry, University of Tübingen, Auf der Morgenstelle 18, 72076 Tübingen, Germany

* Correspondence: juergen.meyer@uni-tuebingen.de

Abstract: The discovery of melamine by Justus von Liebig was fundamental for the development of several fields of chemistry. The vast majority of compounds with melamine or melamine derivatives appear as adducts. Herein, we focus on the development of novel compounds containing anionic melamine species, namely the melaminates. For this purpose, we analyze the reaction of SbCl_3 with melamine by differential scanning calorimetry (DSC). The whole study includes the synthesis and characterization of three antimony compounds that are obtained during the deprotonation process of melamine to melaminates with the reaction sequence from $\text{SbCl}_4(\text{C}_9\text{N}_{18}\text{H}_{19})$ (1) via $(\text{SbCl}_4(\text{C}_6\text{N}_{12}\text{H}_{13}))_2$ (2) to $\text{SbCl}(\text{C}_3\text{N}_6\text{H}_4)$ (3). Compounds are characterized by single-crystal X-ray diffraction (SXRD), powder X-ray diffraction (PXRD), and infrared spectroscopy (IR). The results give an insight into the mechanism of deprotonation of melamine, with the replacement of one, two, or eventually three hydrogen atoms from the three amino groups of melamine. The structure of (3) suggests that metal melaminates are likely to form supramolecular structures or metal-organic frameworks (MOFs).

Keywords: melaminates; antimony; melamine; melaminium; deprotonation; crystal structures



Citation: Bayat, E.; Ströbele, M.; Meyer, H.-J. Unraveling the Synthesis of $\text{SbCl}(\text{C}_3\text{N}_6\text{H}_4)$: A Metal-Melaminates Obtained through Deprotonation of Melamine with Antimony(III)Chloride. *Chemistry* **2023**, *5*, 1465–1476. <https://doi.org/10.3390/chemistry5020099>

Academic Editors: Christoph Janiak, Sascha Rohn and Georg Manolikakes

Received: 4 May 2023

Revised: 12 June 2023

Accepted: 14 June 2023

Published: 20 June 2023



Copyright: © 2023 by the authors. Licensee MDPI, Basel, Switzerland. This article is an open access article distributed under the terms and conditions of the Creative Commons Attribution (CC BY) license (<https://creativecommons.org/licenses/by/4.0/>).

1. Introduction

In the 19th century, the foundation of amine-substituted s-triazine derivatives was laid for the first time by Liebig and Gmelin [1–3] with the synthesis of melamine, melam, melem and their condensation product called melon. Melamine (1,3,5-triazine-2,4,6-triamine) is the simplest and most intensively studied C/N/H compound synthesized from potassium thiocyanate and ammonium chloride for the first time (1834) by Liebig [1,4]. However, it can also be easily achieved with trimerization of cyanamide (CN_2H_2), while today, industrial productions take place from urea in tons [5–7]. Melamine has a relatively high-melting point for an organic compound and undergoes condensation reactions on heating. The condensation products melem, melam, and melon (Figure 1) of this ancestry compound have been studied extensively using various spectroscopy techniques [8,9]. For a long period, thermal condensation was not fully understood due to the chemical inertness and low solubility of these products [10]. In 1959, May conducted a study on the pyrolysis of melamine at temperatures between 200 °C and 500 °C [11]. Afterward, this process was investigated by several scientists, particularly by Schnick and Lotsch [12,13]. The temperature-programmed XRD (TPXRD) was used in the temperature range between 25 °C and 660 °C to clarify the exact temperatures of formation of condensed products, which shows that the sublimation temperature of melamine is approximately 360–370 °C at atmospheric pressure. However, TPXRD in semi-closed systems shows that the X-ray reflections of melamine disappear at 296 °C, and then melamine forms melam and melem, which are stable up to 379 °C [13]. Pure melem, which consists of internally hydrogen-

bonded heptazine molecules, can be obtained at 379 °C and is stable up to 500 °C. The polymeric carbon nitride material melon is also achieved with further heating [13].

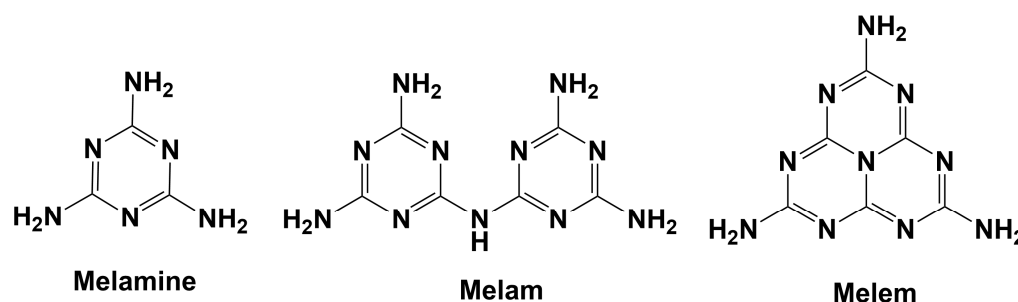


Figure 1. Molecular structures of melamine ($C_3N_6H_6$), melam ($C_6N_{11}H_9$) and melem ($C_6N_{10}H_6$).

In addition to the many applications melamine has, such as surface coating [14], flame redundancy [14–17], and heavy metal removal [18,19], it has some unique characteristics which make it a relevant research topic up to this day. The most important potential of melamine is its ability to create a metal-organic framework (MOF) [20] or porous-organic framework (POFs) [21] by the formation of metal melaminates.

Justus von Liebig's discovery of melamine was essential in the progress of C/N/H chemistry. Most melamine-containing compounds and their derivatives are found as adducts. Cationic C/N/H ions are present in various molecular compounds, including melamine, melam, and melem. These ions are formed by protonating the ring nitrogen atoms, which are more basic than the terminal amino groups. The most common cations are monoprotonated, but di- or trications have also been observed. More research into the chemistry of these substances led to the discovery of melaminium [22–26], melamium, and melemium salts. By far, the majority of salts were produced by melamine, including melaminium sulfate [27], melaminium nitrate, melaminium phosphates [16,28], melaminium chloride [29], organic salts of phthalates [30], benzoates, or citrates [31], and many inorganic salts containing complex anions [32,33]. On the other hand, a small number of melamium salts have been studied, such as melamium bromide and iodide [26]. Recently, melemium salts, namely melemium sulfate, triple protonated melemium methylsulfonate, and melemium perchlorate, are also discovered [34,35]. Melamine was also reported to coordinate with metal halides to form organic-inorganic hybrid copper halides such as $Cu_2Br_2(C_3N_6H_7)_n$, $[Cu_3Cl_3(C_3N_6H_7)]_n$ [36], the silver complex $[Ag(C_3N_6H_6)(H_2O)(NO_3)]_n$, and the mercury compound $(C_3N_6H_7)(C_3N_6H_6)HgCl_3$ [37], which have biochemical applications and nonlinear optical properties [38,39].

Regarding the basic property of melamine, protonation is easy, and a great variety of such compounds, either theoretically or experimentally, have been investigated [25,26,40,41]. A new class of chemistry related to melaminates (deprotonated melamine) has received less attention until now; however, it is very important from either a chemistry or application perspective. The coordination behavior of molecules such as guanidine or melamine, capable of forming extended hydrogen bonds, can be changed by deprotonation [36,42]. Thus, it is a promising strategy for synthesizing interconnected supramolecular structures or MOFs. Despite the challenge which arises from the rigidity of its heterocyclic structure, the affinity of ring-N atoms to act as H-bond acceptors, and the steric hindrance of neighboring amino groups [35], the deprotonation of melamine seems to be plausible since guanidine (a stronger base) has already been deprotonated twice [43]. Franklin pioneered the work on anionic melamine by synthesizing two compounds of $K(C_3N_6H_5) \cdot NH_3$ and $K_3(C_3N_6H_3)$ [44,45] in liquid ammonia. However, these compounds were only characterized using elemental analyses, and no crystallographic structure information was provided. Later, Dronskowski and coworkers confirmed the presence of the two ammonia adducts, $K(C_3N_6H_5) \cdot NH_3$ and $Rb(C_3N_6H_5) \cdot \frac{1}{2}NH_3$ by single-crystal X-ray diffraction. Ammonia-free $K_3(C_3N_6H_3)$ has been assigned by its characteristic infrared bands, being compared with

calculated bands from density-functional theory (DFT) [42]. There was no further research reported on these classes of compounds and their properties until the discovery and identification of the copper melamate $\text{Cu}_3(\text{C}_3\text{N}_6\text{H}_3)$ with a layered framework structure by Meyer & coworkers [20].

In this work, the step-wise deprotonation of melamine in a solid state has been studied by thermal analysis. Herein, antimony (III) chloride is used for the deprotonation of melamine due to its low melting point of $73.4\text{ }^\circ\text{C}$ [46]. The recorded reaction sequence shows three compounds that were prepared and later characterized by powder X-ray diffraction (PXRD), single-crystal diffraction, and IR measurements. The structure of $\text{SbCl}(\text{C}_3\text{N}_6\text{H}_4)$ suggests the potential of synthesizing interconnected supramolecular structures or metal-organic frameworks (MOFs).

2. Materials and Methods

2.1. Materials

The starting materials, melamine (2,4,6-triamino-1,3,5-triazine, purchased from Sigma-Aldrich, 99%), and antimony(III)chloride (Sigma-Aldrich, 99%), ammonium chloride (Sigma-Aldrich, 99.99%) were used without further purification. The reaction mixtures were prepared under an argon atmosphere in a glovebox with moisture and oxygen levels below 1 ppm and transferred into homemade silica tubing (inner diameter 13 mm and 7 mm) and sealed under vacuum. The reactions were carried out in Simon–Müller and Carbolite chamber furnaces.

2.1.1. Synthesis

Synthesis of $\text{SbCl}_4(\text{C}_9\text{N}_{18}\text{H}_{19})$ (1):

Precursors were pestled in an agate mortar with a 1:4 molar ratio of antimony(III)chloride and melamine. A mixture of antimony(III) chloride and melamine with a total mass of ≈ 200.0 mg was transferred into a homemade silica ampule and sealed therein under vacuum. The ampoule was placed into a Simon–Müller furnace and heated to $200\text{ }^\circ\text{C}$ for 20 h with a heating rate of $2\text{ }^\circ\text{C}/\text{min}$ and cooling ramp of $0.5\text{ }^\circ\text{C}/\text{min}$ (Figure S1). The reaction produced a white color product crystallized on the top of the ampule ($>90\%$ yield w.r.t Sb). A temperature gradient seemed to play an essential role in the separation of the product (1).

The solubility of compound (1) has been investigated in acetonitrile, THF, DCM, ethanol, methanol, and water. The PXRD measurements showed the decomposition of this product to unknown phases.

Synthesis of $(\text{SbCl}_4(\text{C}_6\text{N}_{12}\text{H}_{13}))_2$ (2):

Similar to the previous preparation, the mixture of antimony (III)chloride and melamine was mixed in a 1:2 molar ratio (total mass of ≈ 200.0 mg) and heated to $200\text{ }^\circ\text{C}$ for 20 h with a heating and cooling rate of $2\text{ }^\circ\text{C}/\text{min}$ (Figure S1). The product was X-ray amorphous powder and contained transparent single crystals of (2) (10% w.r.t Sb).

Synthesis of $\text{SbCl}(\text{C}_3\text{N}_6\text{H}_4)$ (3):

The structure of (3) was obtained from both (1:2 and 1:4) ratios of antimony(III)chloride and melamine by heating the 1:2 ratio at $250\text{ }^\circ\text{C}$ for 20 h, or by heating the 1:4 ratio at $280\text{ }^\circ\text{C}$ for 20 h (Figure S1). The beige color product was isolated in 50% yield w.r.t Sb.

The solubility of compound (3) has been studied in many solvents. The powder was soaked for one hour in acetonitrile, THF, DMF, DCM, ethanol, methanol, water, and diluted acetic acid. Subsequent PXRD measurements were undertaken. The results showed that compound (3) remains stable in acetonitrile, THF, DMF, DCM, ethanol, and methanol. However, in water and DMSO, compound (3) decomposes and forms Sb_2O_3 and an unknown phase, respectively. The schematic synthesis of all three compounds is presented in Figure S1.

2.1.2. X-ray Powder Diffraction

The X-ray diffraction of prepared powders was recorded with a powder diffractometer (STOE Darmstadt, STADIP, Ge-monochromator) using $\text{Cu-K}_{\alpha 1}$ ($\lambda = 1.540598\text{ \AA}$) radiation

in the range of $5 < 2\theta < 120^\circ$. Match3! Software [47] was used to compare the patterns with patterns of the corresponding crystal structures.

2.1.3. Single-Crystal X-ray Diffraction

Single Crystals of (1), (2), and (3) were selected and placed on a single-crystal X-ray diffractometer (Rigaku XtaLab Synergy-S) with Cu-K α radiation ($\lambda = 1.54184 \text{ \AA}$) and a mirror monochromator at 150 or 220 K. Crystal structures were solved by direct methods (SHELXT) [48], followed by full-matrix least-squares structure refinements (SHELXL-2014) [49]. The absorption correction of X-ray intensities was performed with numerical methods using the CrysAlisPro 1.171.41.92a software (Rigaku Oxford Diffraction). Hydrogen atoms were found in the difference map and refined therefrom isotropically.

2.1.4. Thermoanalytic Studies

Differential scanning calorimetry (DSC) was carried out using a DSC 204 F1 Phoenix (Fa. Netzsch, Selb, Germany). The starting materials were enclosed under Ar in a glovebox into gold-plated (5 μm) steel autoclaves with a volume of 100 μL (Bächler Feintech AG in Hölstein, Switzerland). The reactions of SbCl $_3$ with melamine were analyzed for different ratios between room temperature and 500 $^\circ\text{C}$ at a heating and cooling rate of 2 $^\circ\text{C}/\text{min}$.

2.1.5. Infrared Spectra

The infrared (IR) spectra of samples were recorded with a Bruker VERTEX 70 FT-IR spectrometer within the spectra range of 400–4000 cm^{-1} . Tablets of KBr were used as a background.

3. Results and Discussion

3.1. Thermoanalytic Studies

Thermal analyses based on DSC and DTA have been shown to be highly insightful regarding the examination of reaction sequences [50,51] and for comprehensive studies of binary or ternary systems [52], especially when combined with PXRD studies. Following this method, the formation or decomposition of a crystalline species is usually indicated by a thermal event, and the newly formed species is characterized by X-ray diffraction techniques.

The differential scanning calorimetric (DSC) measurements of 1:2 and 1:4 molar mixtures of antimony chloride and melamine are shown in Figure 2, with heating and cooling rates of 2 $^\circ\text{C}/\text{min}$. The DSC patterns display a small exothermic peak at around 70 $^\circ\text{C}$, which can be attributed to the melting point of antimony(III)chloride. Figure 2a,b show multiple exothermic effects between 200 $^\circ\text{C}$ and 300 $^\circ\text{C}$. The resolution of thermal events in this region is rather poor and cannot be significantly improved by changing the heating ramp. For example, we have explored different heating rates throughout. At lower heating rates, the signals were smeared out and were not as sharp as the signals shown in Figure 2a,b, so the resolution was worse. The presented heating rate is the optimized heating rate with respect to the signal-to-noise ratio. Moreover, the effects are slightly different for different ratios of starting materials, with lower reaction temperatures in the presence of more melamine.

Powder XRD patterns were recorded on samples obtained under conditions given in the DSC experiments, being interrupted at certain temperatures, especially in the temperature region between 200 $^\circ\text{C}$ and 280 $^\circ\text{C}$. Compound (1) was already formed at 200 $^\circ\text{C}$ from a 1:4 ratio of starting materials, and compound (2) was observed in the XRD pattern from a 1:2 ratio at the same temperature. Compound (3) was identified at around 280 $^\circ\text{C}$ from a 1:4 ratio of starting materials or, alternatively, at 250 $^\circ\text{C}$ from a 1:2 ratio. The endothermic peaks at 370 $^\circ\text{C}$ indicate the melting/decomposition of (excess) melamine, which appears sharper for the 1:4 ratio due to the larger amount of melamine. This assignment is confirmed by a DSC of melamine (Figure S2), which shows a similar endothermic peak with a slight shift at 361 $^\circ\text{C}$. At slightly higher temperatures, compound (3) is decomposed, which is followed by a strong exothermic peak at 400 $^\circ\text{C}$ and 417 $^\circ\text{C}$ for the 1:4 and a 1:2 ratio, respectively.

These intense exothermic peaks led to the formation of a phase with a yellow color (4) that looked glassy under the microscope. This was further studied by means of IR spectroscopy (see the relevant section).

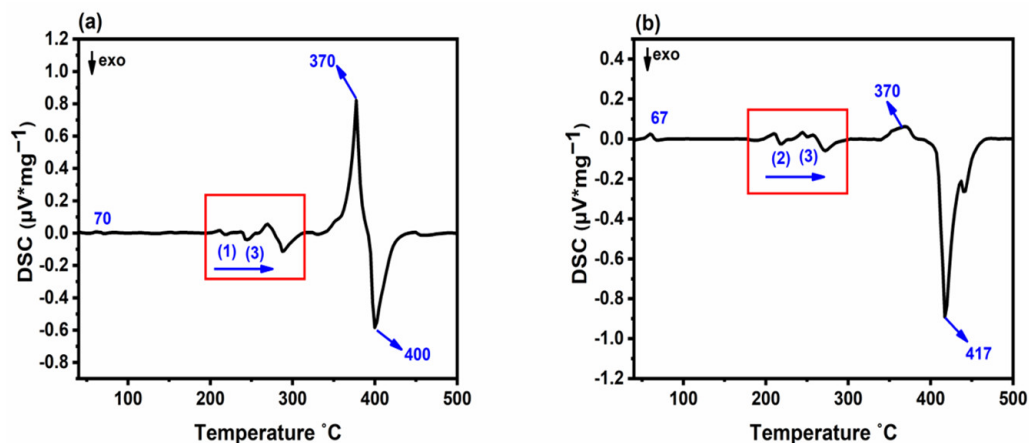


Figure 2. (a) DSC of the reaction of SbCl_3 and melamine in a ratio of 1:4, (b) DTA of the reaction of SbCl_3 and melamine in a ratio of 1:2.

From this study, we note that reactions in the given system proceed very quickly, almost simultaneously, making the assignment of compounds and their preparations challenging. This is due to the high reactivity of reaction partners.

3.2. Crystal Structures

Crystal structures of all three compounds (1), (2), and (3) were solved and refined based on single-crystal X-ray diffraction data with triclinic ($P\bar{1}$) and monoclinic ($P2_1/c$ and $P2_1/n$) space groups, respectively, with crystallographic details summarized in Table 1 and relevant distances given in Table 2. The asymmetric unit of each compound is shown in Figure S3.

The crystal structure of (1) is composed of one deprotonated melamine, two protonated melamine and a single chloride ion besides SbCl_3 to make up $\text{SbCl}_4(\text{C}_3\text{N}_6\text{H}_5)(\text{C}_3\text{N}_6\text{H}_7)_2$. The crystal structure contains a sequence of three distinct layers stacked on top of each other (along b); one of them is displayed in Figure 3. Stacking behavior is most common for melamine-based structures.

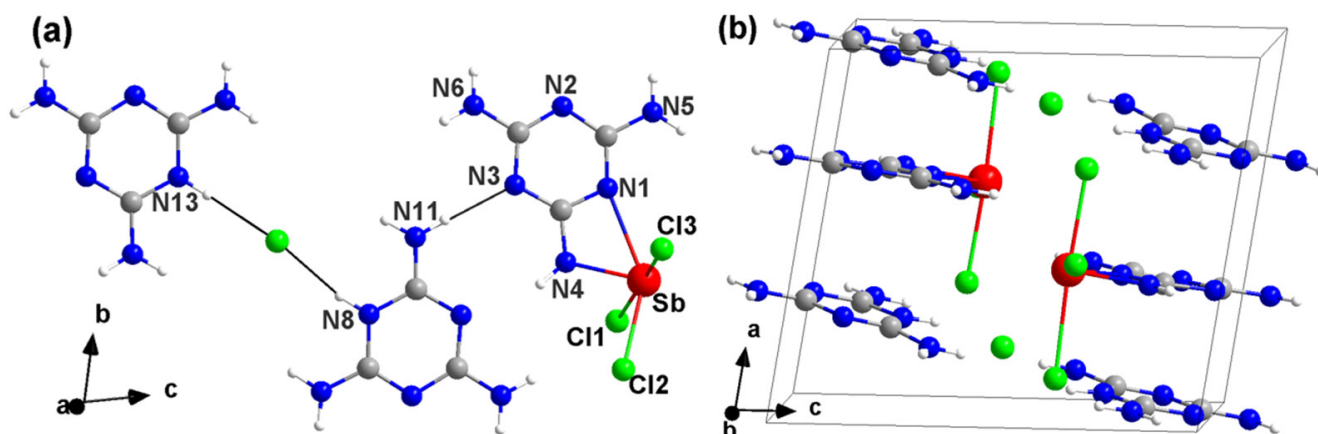


Figure 3. (a) Constituents of one layer in the structure of (1) as $\text{SbCl}_4(\text{C}_3\text{N}_6\text{H}_5)(\text{C}_3\text{N}_6\text{H}_7)_2$, and (b) a perspective view of the unit cell of (1) along the b -axis, with the color code: N: blue, C: gray, H: white, Cl: green, Sb: red).

Table 1. Crystallographic details of the crystal structure refinement of compounds (1), (2), and (3).

Compound	(1)	(2)	(3)
CCDC code	2201273	2210244	2213381
Formula weight	642.97	1033.67	281.32
Temperature/K	220.0(1)	150.0(1)	150.0(1)
Wavelength/Å	1.54184	1.54184	1.54184
Space group	$P\bar{1}$	$P2_1/c$	$P2_1/n$
$a/\text{Å}$	9.5878(5)	13.2780(2)	5.3562(2)
$b/\text{Å}$	10.5395(3)	10.6878(1)	10.5432(3)
$c/\text{Å}$	11.4338(5)	24.0953(2)	12.5618(4)
$\alpha/^\circ$	74.011(3)	90	90
$\beta/^\circ$	79.122(4)	105.860(1)	93.710(3)
$\gamma/^\circ$	85.602(3)	90	90
Volume/Å ³	1090.37(8)	3289.26(7)	707.90(4)
Z	2	4	4
R_{int}	0.0364	0.0485	0.0312
Goodness-of-fit on F^2	1.074	1.044	1.044
wR_2 (all data)	0.0660	0.0607	0.0267
wR_2	0.0643	0.0603	0.0264
Final R indices (all data)	0.0339	0.0251	0.0120
R_1	0.0278	0.0243	0.0110
$\theta_{\text{Max.}}/^\circ$	4.365	3.460	5.483
$\theta_{\text{Min.}}/^\circ$	66.585	66.583	70.067
μ/mm^{-1}	14.93	19.478	33.932
$\Delta\rho_{\text{Max.}}/e\cdot\text{Å}^{-3}$	0.508	2.491	0.322
$\Delta\rho_{\text{Min.}}/e\cdot\text{Å}^{-3}$	−0.593	−0.597	−0.451
Completeness/%	97.3	100	99.8

Table 2. Selected interatomic distances (pm) of compounds (1), (2), and (3).

Compound (1)			Compound (2)			Compound (3)		
Atom	Atom	Length/pm	Atom	Atom	Length/pm	Atom	Atom	Length/pm
Sb1	Cl1	276.5(8)	Sb1	Cl3	284.7(6)	Sb1	N2	241.5(1)
Sb1	N1	253.6(3)	Sb1	Cl4	260.6(0)	Sb1	N6	208.6(8)
Sb1	Cl2	247.0(0)	Sb1	Cl5	248.7(2)	Sb1	N4	204.4(6)
Sb1	Cl3	256.8(2)	Sb1	Cl1	240.2(1)	Sb1	Cl1	254.9(3)
Sb1	N4	204.7(3)	Sb2	N1	256.1(3)			
			Sb2	N4	204.7(3)			
			Sb2	Cl6	279.2(7)			
			Sb2	Cl7	247.2(8)			
			Sb2	Cl8	251.1(1)			

The SbCl_3 entity in the structure, with its lone pair, is well known from several crystal structures having average Sb–Cl distances of 260.1 pm [53]. The antimony is connected with an exocyclic nitrogen atom of the melaminic ion ($\text{C}_3\text{H}_5\text{N}_6$)[−] via Sb–N4 (204.7(3) pm) and an obviously weaker interaction via Sb–N1 (253.6(3) pm). The constituents in each layer in (1) are interconnected by a network of hydrogen bonds (Figure 3a). An isolated Cl^- ion in the structure is interconnected by hydrogen bridges at $d_{\text{H-Cl}} = 216.3$ pm and 225.6 pm, consistent with the corresponding value in melaminium chloride $d_{\text{H-Cl}} = 239.7$ pm [29].

The crystal structure of (2) comprises one deprotonated melamine, three protonated melaminium ions, an SbCl_3 unit and an $(\text{SbCl}_5)^{2-}$ ion to make up $(\text{SbCl}_4)_2(\text{C}_3\text{N}_6\text{H}_5)(\text{C}_3\text{N}_6\text{H}_7)_3$ displayed in Figure 4. The average Sb–Cl distances in SbCl_3 are 259.3 pm, and those of SbCl_5 are 262.1 pm and 257.8 pm, supporting the presence of Sb^{3+} throughout. Antimony in SbCl_3 is interconnected with the melaminic ion ($\text{C}_3\text{H}_5\text{N}_6$)[−] via Sb–N4 (204.4(6) pm) and an obviously

weaker interaction via Sb-N1 (256.1(3) pm). Again, the crystal structure features a layered arrangement and hydrogen bridging within layers.

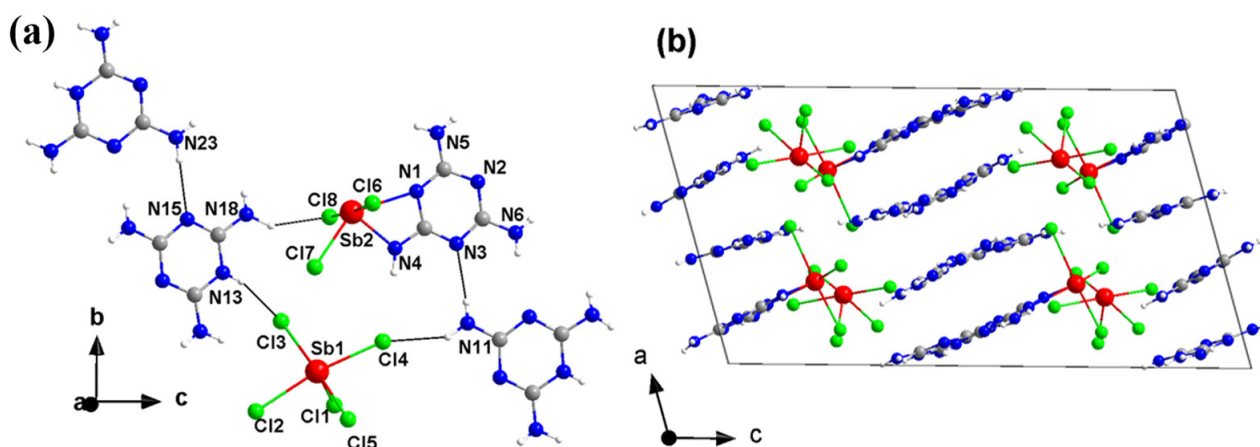


Figure 4. (a) Section of the crystal structure of (2) as $(\text{SbCl}_4)_2(\text{C}_3\text{N}_6\text{H}_5)(\text{C}_3\text{N}_6\text{H}_7)_3$ projected on the bc -plane, and (b) a perspective view along the b -axis with the color code: N: blue, C: gray, H: white, Cl: green, Sb: red).

The crystal structure of (3) features the presence of $(\text{SbCl}_4)^{2+}$ and the melamine ion $(\text{C}_3\text{N}_6\text{H}_4)^{2-}$ in $\text{SbCl}(\text{C}_3\text{N}_6\text{H}_4)$. Unlike the two previous systems, this structure can be described as an infinite chain structure due to the bridging connectivity of the divalent melamine anion, all shown in Figure 5. The $(\text{SbCl}_4)^{2+}$ ($d_{\text{Sb-Cl}} = 254.9(3)$ pm) is interconnected via exocyclic nitrogen atoms of two melamine ions via Sb-N4 (204.4(6) pm) and Sb-N6 (208.6(8) pm) interactions and an obviously weaker interaction via Sb-N2 (241.5(1) pm).

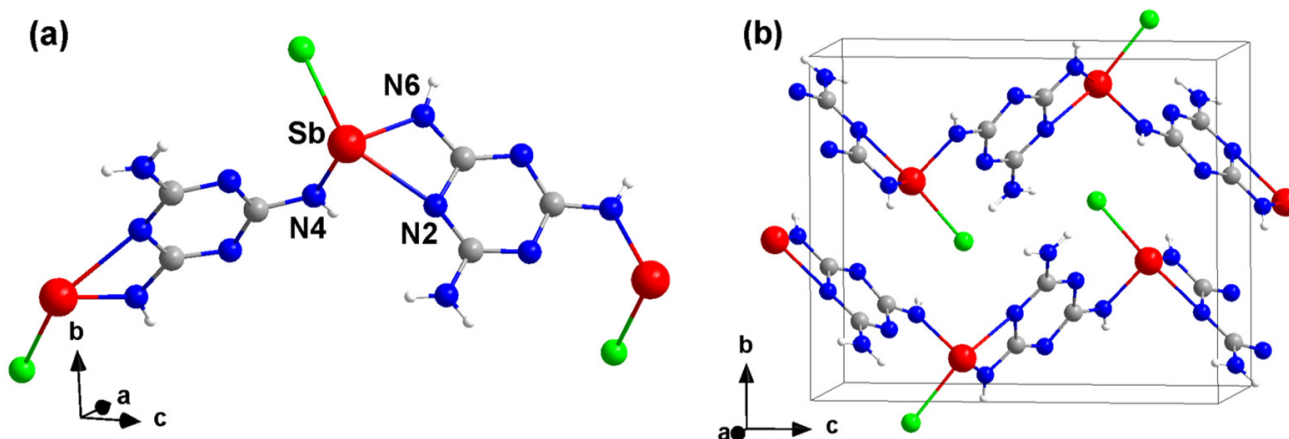


Figure 5. (a) Section of a chain section of the crystal structure of (3) and (b) a perspective view of the unit cell roughly along the a -axis with the color code: N: blue, C: gray, H: white, Cl: green, Sb: red.

The stacking sequences of layers are often dominated by the preference that the N atom of the triazine ring in one layer is alternating with a C atom of the triazine ring in the next layer, which is a characteristic feature in copper melamine [20] and metal cyanurates as well [54,55]. This is achieved by rotating or shifting C_3N_3 units in adjacent layers relative to each other. However, this is not apparent in the structure of compounds (1–3). Layered arrangements of C_3N_3 units are quite clearly visible in compounds (1) and (2) but not in compound (3) (Figures S3–S6). Hence there is the possibility of π - π interactions between C_3N_3 units in (1) and (2). Such interactions can play a crucial role in the stabilization of parallel and antiparallel ring architectures in the crystal structure. The centroid-to-centroid

distance at which C_3N_3 rings may be considered representative of π - π stacking interactions is 360–390 pm in compounds (1) and (2). This distance increases to 560–590 pm in (3) which might present no π - π interactions between layers in this structure.

The range from 357–393 pm was previously reported for several compounds [38,56,57]; for example, in a zinc(II) complex containing melamine (392.8 pm) [56]. In many other studies of copper halide complexes (357.2–389.2 pm), we can see the stacking behavior of twisted melamine rings, which represents the π - π interactions [58].

3.3. X-ray Powder Diffraction and Infrared Spectroscopy

The reaction products were investigated by PXRD, and the XRD patterns of (1), and (3) are provided in Figures S7 and S8. Therein, the recorded data are compared with the calculated patterns obtained from the structure refinement based on single-crystal data. Compound (2) was obtained in low yield; therefore, no powder pattern of this intermediate could be recorded. This compound was always found in the presence of (3) or melamine at higher and lower temperatures, respectively. The powder pattern of compound (3) in Figure S8 shows some unidentified diffraction peaks.

3.4. Infrared Spectroscopy (IR)

The IR spectrum of (1), (3) and (4) has been compared to that of melamine and melaminium chloride, as presented in Figure 6. Table S1 lists the frequencies associated with each vibrational mode of these molecules, along with the corresponding bond assignments. Three IR absorption bands, indicative of the asymmetric and symmetric stretching of $-NH_2$ groups of melamine, can be found in the 3500–3300 cm^{-1} range of the melamine spectrum [29,59]. These vibrations can overlap with the $-NH^+$ in melaminium chloride, and due to coupling, the peak is broadened [60]. The characteristic bands of $-NH_2$ groups and $-NH^+$ are also seen in the spectrum of compound (1) at 3462, 3357, and 3433 cm^{-1} . We can see that the first peak (3462 cm^{-1}) in compound (1) is shifted to lower wavenumbers when compared to melamine. This shift may be due to the presence of protonated melamine units in (1). In fact, the presence of hydrogen bonding would shift $-NH_2$ IR bands to lower wavenumbers, as the hydrogen bond would weaken the NH_2 bond and lower its vibrational frequency [61]. However, due to coupling with the $N-H \cdots Cl$ stretching mode or the presence of heavier atoms (Cl, Sb) in compound (1), the second peak (3357 cm^{-1}) is shifted to slightly higher wavenumbers and also broadened [29]. Similarly, infrared spectra for compounds (3) and (4) indicate that the asymmetric and symmetric vibrations of $-NH_2$ overlap with those of $-NH^+$ in both compounds, as evidenced by the disappearance of the first peak (3471 cm^{-1} for melamine) and the broadening of the other two peaks. The bending mode bands for melaminium chloride and compound (1) are substantially higher than those for melamine (1652 cm^{-1}) at 1722, 1676, 1649 cm^{-1} and 1679, 1656, and 1612 cm^{-1} , respectively. This is explained by the fact that melaminium chloride and (1) have fewer intermolecular interactions than melamine. In compounds (3) and (4), bending modes are split into multiple bands, showing that $-NH_2$ groups in these compounds have different vibrational frequencies due to the presence of neighboring atoms and molecular interactions in these structures. The region below 1500 cm^{-1} is related to C-N, and C=N ring stretching modes, C-N side group stretching, N-H rocking, and triazine ring breath and bending vibrations, which are listed with detailed numbers in Table S1. The exact position of these peaks can depend on various factors, such as the substitution pattern of the triazine ring and the nature of the surrounding chemical environment, which agrees well with the slight shifts in each region for compounds (1), (3), and (4). The strong split-band at 800 cm^{-1} , which is brought on by the sextant-bend of both the triazine and heptazine rings, provides additional evidence that compound (4) is still either a heptazine- or triazine-based compound (IR cannot differentiate between triazine and heptazine) [13,22,62], whereas the yellow emission color of the compound under ultraviolet radiation rather indicates a heptazine based compound.

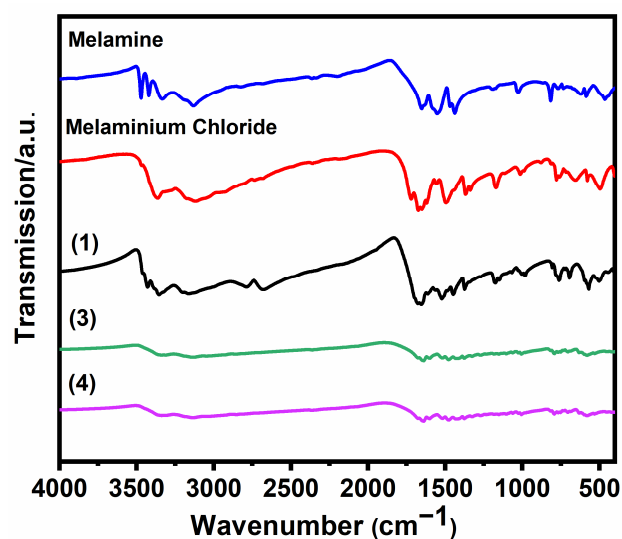


Figure 6. FTIR spectrum of melamine, melaminium chloride powder, compared with compounds (1), (3), (4).

4. Conclusions

The development of metal melaminates is just at its beginning. A preparative concept for the development of melaminates was recently established for $\text{Cu}_3(\text{C}_3\text{H}_3\text{N}_3)$ based on the reaction of CuCl with melamine. The same concept is employed in this study for the reaction of SbCl_3 with melamine. Thermal studies (DSC) reveal a narrow sequence of thermal events, or rather intertwining reactions that reveal new compounds, following the sequence (1), (2) and (3) with increasing temperature.

Indeed, the final product of the given reaction cascade is compound (3), observed via compounds (1) and (2). For a better description of the reaction sequence of compounds, we use the abbreviation *Mel* for melamine, with $\text{Mel}^{(n-)}$ for melamate and $\text{Mel}^{(+)}$ for melaminium. The overall reaction representing the formation of compound (3) can be described as follows:



The formation of HCl in this reaction can be equivalent to melaminium chloride ($\text{Mel}^{(+)}\text{Cl}$), which is, in fact, present in compound (1) but is lost at elevated temperatures through sublimation, which indeed has been reported as a side-phase for the corresponding reaction of CuCl and melamine [20]. This reaction scheme with metal halide and melamine is indeed a useful way to develop metal melaminates. However, reactions with melamine are intrinsically difficult due to the high reactivity and condensation behavior of melamine.

The reaction of SbCl_3 with excess melamine passes through some intermediate reaction stages with the formations of melamine derivatives (Mel^- , Mel^+) that are successively lost with increasing temperature from (1) to (2) and finally (3). Compound (1) is best described as $\text{SbCl}_4\text{Mel}^{(-)}(\text{Mel}^{(+)})_2$ containing three melamine species per antimony atom, and compound (2) is given as $(\text{SbCl}_4)_2\text{Mel}^{(-)}(\text{Mel}^{(+)})_3$ and contains only two melamine derivatives per antimony atom until only one melamate is left in (3). The formation of the expectable compound $\text{SbMel}^{(3-)}$ is not observed.

Supplementary Materials: The following supporting information can be downloaded at: <https://www.mdpi.com/article/10.3390/chemistry5020099/s1>, Reference [29] is also cited in the supplementary materials.

Author Contributions: Conceptualization, supervision, funding acquisition, review and editing, H.-J.M.; Synthesis, PXRD and IR, writing, E.B.; X-ray diffraction refinements and structure solutions, M.S. All authors have read and agreed to the published version of the manuscript.

Funding: This research received no external funding.

Data Availability Statement: Data is contained within the article and Supplementary Materials.

Acknowledgments: A sincere thank you to Mike Healey Smith for his diligent English revisions and proofreading of this article.

Conflicts of Interest: The authors declare no conflict of interest.

References

1. Liebig, J. Über einige Stickstoff-Verbindungen. *Ann. Pharm. Fr.* **1834**, *10*, 1–47. [[CrossRef](#)]
2. Gmelin, L. Über einige Verbindungen des Melon's. *Ann. Pharm. Fr.* **1835**, *15*, 252–258. [[CrossRef](#)]
3. Liebig, J. Über die Constitution der Mellonverbindungen. *Justus Liebigs Ann. Chem.* **1855**, *95*, 257–282. [[CrossRef](#)]
4. Finkel'shtein, A.; Boitsov, E. The molecular structure of 1,3,5-triazine and its derivatives. *Russ. Chem. Rev.* **1962**, *31*, 712. [[CrossRef](#)]
5. Crews, G.M.; Ripperger, W.; Kersebohm, D.B.; Güthner, T.; Mertschenk, B. Melamine and guanamines. In *Ullmann's Encyclopedia of Industrial Chemistry*; Wiley: Weinheim, Germany, 2001. [[CrossRef](#)]
6. Kefler, F.K. Structure and Reactivity of S-Triazine-Based Compounds in C/N/H Chemistry. Ph.D. Thesis, Ludwig Maximilian University of Munich, Munich, Germany, 2019.
7. Klason, P. Über Melamverbindungen. *J. Prakt. Chem.* **1886**, *33*, 285–289. [[CrossRef](#)]
8. Finkel'shtein, A.I.; Spiridonova, N.Y.V. Chemical properties and molecular structure of derivatives of sym-heptazine [1,3,4,6,7,9,9b-heptaazaphenalene, tri-1,3,5-triazine]. *Russ. Chem. Rev.* **1964**, *33*, 400. [[CrossRef](#)]
9. Jürgens, B.; Irran, E.; Senker, J.; Kroll, P.; Müller, H.; Schnick, W. Melem (2,5,8-Triamino-tri-s-triazine), an Important Intermediate during Condensation of Melamine Rings to Graphitic Carbon Nitride: Synthesis, Structure Determination by X-ray Powder Diffractometry, Solid-State NMR, and Theoretical Studies. *J. Am. Chem. Soc.* **2003**, *125*, 10288–10300. [[CrossRef](#)]
10. Kroke, E.; Schwarz, M. Novel group 14 nitrides. *Coord. Chem. Rev.* **2004**, *248*, 493–532. [[CrossRef](#)]
11. May, H. Pyrolysis of melamine. *J. Appl. Chem.* **1959**, *9*, 340–344. [[CrossRef](#)]
12. Sattler, A.; Pagano, S.; Zeuner, M.; Zurawski, A.; Gunzelmann, D.; Senker, J.; Müller-Buschbaum, K.; Schnick, W. Melamine–melem adduct phases: Investigating the thermal condensation of melamine. *Chem.-Eur. J.* **2009**, *15*, 13161–13170. [[CrossRef](#)]
13. Lotsch, B.V.; Schnick, W. New light on an old story: Formation of melam during thermal condensation of melamine. *Chem.-Eur. J.* **2007**, *13*, 4956–4968. [[CrossRef](#)] [[PubMed](#)]
14. Weil, E.D. Fire-Protective and Flame-Retardant Coatings—A State-of-the-Art Review. *J. Fire Sci.* **2011**, *29*, 259–296. [[CrossRef](#)]
15. Schartel, B.; Weiß, A.; Mohr, F.; Kleemeier, M.; Hartwig, A.; Braun, U. Flame retarded epoxy resins by adding layered silicate in combination with the conventional protection-layer-building flame retardants melamine borate and ammonium polyphosphate. *J. Appl. Polym. Sci.* **2010**, *118*, 1134–1143. [[CrossRef](#)]
16. Yang, H.; Song, L.; Tai, Q.; Wang, X.; Yu, B.; Yuan, Y.; Hu, Y.; Yuen, R.K.K. Comparative study on the flame retarded efficiency of melamine phosphate, melamine phosphite and melamine hypophosphite on poly(butylene succinate) composites. *Polym. Degrad. Stab.* **2014**, *105*, 248–256. [[CrossRef](#)]
17. Weil, E.D.; Levchik, S.V. Flame Retardants in Commercial Use or Development for Textiles. *J. Fire Sci.* **2008**, *26*, 243–281. [[CrossRef](#)]
18. Yin, N.; Wang, K.; Xia, Y.a.; Li, Z. Novel melamine modified metal-organic frameworks for remarkably high removal of heavy metal Pb(II). *Desalination* **2018**, *430*, 120–127. [[CrossRef](#)]
19. Cao, Y.; Huang, J.; Li, Y.; Qiu, S.; Liu, J.; Khasanov, A.; Khan, M.A.; Young, D.P.; Peng, F.; Cao, D.; et al. One-pot melamine derived nitrogen doped magnetic carbon nanoadsorbents with enhanced chromium removal. *Carbon* **2016**, *109*, 640–649. [[CrossRef](#)]
20. Kallenbach, P.; Bayat, E.; Ströbele, M.; Romao, C.P.; Meyer, H.-J. Tricopper Melaminates, a Metal-Organic Framework Containing Dehydrogenated Melamine and Cu-Cu Bonding. *Inorg. Chem.* **2021**, *60*, 16303–16307. [[CrossRef](#)]
21. Pareek, K.; Rohan, R.; Cheng, H. Polymeric organo–magnesium complex for room temperature hydrogen physisorption. *RSC Adv.* **2015**, *5*, 10886–10891. [[CrossRef](#)]
22. Kessler, F.K.; Schuhbeck, A.M.; Schnick, W. Melamium Thiocyanate Melam, a Melamium Salt with Disordered Anion Sites. *Z. Anorg. Allg. Chem.* **2019**, *645*, 840–847. [[CrossRef](#)]
23. Sattler, A.; Schnick, W. Preparation and Structure of Melemium Melem Perchlorate $\text{HC}_6\text{N}_7(\text{NH}_2)_3\text{ClO}_4 \cdot \text{C}_6\text{N}_7(\text{NH}_2)_3$. *Z. Anorg. Allg. Chem.* **2008**, *634*, 457–460. [[CrossRef](#)]
24. Sattler, A.; Schnick, W. Melemium Hydrogensulfate $\text{H}_3\text{C}_6\text{N}_7(\text{NH}_2)_3(\text{HSO}_4)_3$ —The First Triple Protonation of Melem. *Z. Anorg. Allg. Chem.* **2010**, *636*, 2589–2594. [[CrossRef](#)]
25. Vella-Zarb, L.; Braga, D.; Guy Orpen, A.; Baisch, U. The influence of hydrogen bonding on the planar arrangement of melamine in crystal structures of its solvates, cocrystals and salts. *CrystEngComm* **2014**, *16*, 8147–8159. [[CrossRef](#)]
26. Kessler, F.K.; Koller, T.J.; Schnick, W. Synthesis and Structure of Melamium Bromide $\text{C}_6\text{N}_{11}\text{H}_{10}\text{Br}$ and Melamium Iodide $\text{C}_6\text{N}_{11}\text{H}_{10}\text{I}$. *Z. Anorg. Allg. Chem.* **2018**, *644*, 186–192. [[CrossRef](#)]
27. Braml, J.; Perpétuo, G.J. Bis (melaminium) sulfate dihydrate. *Acta Crystallogr. Sect. C Cryst. Struct. Commun.* **2001**, *57*, 1431–1433. [[CrossRef](#)]
28. Volfkovi, S.I.; Feldmann, W.W.; Kozmina, M.L. Über Kondensierte Phosphate des Melamins. *Z. Anorg. Allg. Chem.* **1979**, *457*, 20–30. [[CrossRef](#)]
29. Janczak, J.; Perpétuo, G.J. Melaminium chloride hemihydrate. *Acta Crystallogr. Sect. C Cryst. Struct. Commun.* **2001**, *57*, 1120–1122. [[CrossRef](#)] [[PubMed](#)]

30. Janczak, J.; Perpétuo, G.J. Melaminium phthalate. *Acta Crystallogr. Sect. C Cryst. Struct. Commun.* **2001**, *57*, 123–125. [[CrossRef](#)]
31. Marchewka, M.; Pietraszko, A. Structure and spectra of melaminium citrate. *J. Phys. Chem. Solids* **2003**, *64*, 2169–2181. [[CrossRef](#)]
32. Colombo, A.; Menabue, L.; Motori, A.; Pellacani, G.C.; Porzio, W.; Sandrolini, F.; Willett, R. Crystal structure and spectroscopic, magnetic, and electrical properties of a copper (II) dimer, melaminium hexachlorodocuprate, exhibiting a new stacking interaction. *Inorg. Chem.* **1985**, *24*, 2900–2905. [[CrossRef](#)]
33. Kroenke, W.J.; Fackler, J.P., Jr.; Mazany, A.M. Structure and bonding of melaminium. beta-octamolybdate. *Inorg. Chem.* **1983**, *22*, 2412–2416. [[CrossRef](#)]
34. Sattler, A.; Seyfarth, L.; Senker, J.; Schnick, W. Synthesen, Kristallstrukturen und spektroskopische Eigenschaften des Melem-Adduktes $C_6N_7(NH_2)_3 \cdot H_3PO_4$ sowie der Melemium-Salze $(H_2C_6N_7(NH_2)_3)SO_4 \cdot 2H_2O$ und $(HC_6N_7(NH_2)_3)ClO_4 \cdot H_2O$. *Z. Anorg. Allg. Chem.* **2005**, *631*, 2545–2554. [[CrossRef](#)]
35. Sattler, A.; Schönberger, S.; Schnick, W. Melemium Methylsulfonates $HC_6N_7(NH_2)_3H_2C_6N_7(NH_2)_3(SO_3Me)_3 \cdot H_2O$ and $H_2C_6N_7(NH_2)_3(SO_3Me)_2 \cdot H_2O$. *Z. Anorg. Allg. Chem.* **2010**, *636*, 475–482. [[CrossRef](#)]
36. Zhang, L.; Zhang, J.; Li, Z.-J.; Cheng, J.-K.; Yin, P.-X.; Yao, Y.-G. New Coordination Motifs of Melamine Directed by N–H...X (X=Cl or Br) Hydrogen Bonds. *Inorg. Chem.* **2007**, *46*, 5838–5840. [[CrossRef](#)]
37. Rana, A.; Bera, M.; Chowdhuri, D.S.; Hazari, D.; Jana, S.K.; Zangrando, E.; Dalai, S. 3D Coordination Network of Ag(I) Ions with μ_3 -Bridging Melamine Ligands. *J. Inorg. Organomet. Polym. Mater.* **2012**, *22*, 360–368. [[CrossRef](#)]
38. Bai, Z.; Lee, J.; Kim, H.; Hu, C.L.; Ok, K.M. Unveiling the Superior Optical Properties of Novel Melamine-Based Nonlinear Optical Material with Strong Second-Harmonic Generation and Giant Optical Anisotropy. *Small*, **2023**; *in press*. [[CrossRef](#)] [[PubMed](#)]
39. Liu, L.; Wu, Y.; Ma, L.; Fan, G.; Gao, W.; Wang, W.; Ma, X. A new melamine-based Cu(I) coordination polymer with an excellent photocatalytic activity, therapeutic and nursing effects on the blood glucose regulation. *J. Struct. Chem.* **2022**, *63*, 302–309. [[CrossRef](#)]
40. Braml, N.E.; Sattler, A.; Schnick, W. Formation of melaminium adducts by pyrolysis of thiourea or melamine/ NH_4Cl mixtures. *Chem.-Eur. J.* **2012**, *18*, 1811–1819. [[CrossRef](#)] [[PubMed](#)]
41. Mukherjee, S.; Ren, J. Gas-phase acid-base properties of melamine and cyanuric acid. *J. Am. Soc. Mass Spectrom.* **2010**, *21*, 1720–1729. [[CrossRef](#)]
42. Gorne, A.L.; Scholz, T.; Kobertz, D.; Dronskowski, R. Deprotonating Melamine to Gain Highly Interconnected Materials: Melamate Salts of Potassium and Rubidium. *Inorg. Chem.* **2021**, *60*, 15069–15077. [[CrossRef](#)]
43. Gorne, A.L.; George, J.; van Leusen, J.; Duck, G.; Jacobs, P.; Chogondahalli Muniraju, N.K.; Dronskowski, R. Ammonothermal Synthesis, Crystal Structure, and Properties of the Ytterbium(II) and Ytterbium(III) Amides and the First Two Rare-Earth-Metal Guanidates, $YbC(NH)_3$ and $Yb(CN_3H_4)_3$. *Inorg. Chem.* **2016**, *55*, 6161–6168. [[CrossRef](#)]
44. Franklin, E.C. The ammono carbonic acids. *J. Am. Chem. Soc.* **1922**, *44*, 486–509. [[CrossRef](#)]
45. Schnick, W.; Huppertz, H. Darstellung, Kristallstruktur und Eigenschaften von Kaliumhydrogencyanamid. *Z. Anorg. Allg. Chem.* **1995**, *621*, 1703–1707. [[CrossRef](#)]
46. Haynes, W.M. *CRC Handbook of Chemistry and Physics*, 95th ed.; CRC Press LLC: Boca Raton, FL, USA, 2016.
47. Putz, H.; Brandenburg, K. *Match!—Phase Analysis Using Powder Diffraction, Version 3.15.x*; Crystal Impact: Bonn, Germany, 2023.
48. Sheldrick, G.M. *SHELXS-97 and SHELXL-97, Program for Crystal Structure Solution and Refinement*; University of Göttingen: Göttingen, Germany, 1997.
49. Dolomanov, O.; Bourhis, L.; Gildea, R.; Howard, J.; Puschmann, H. OLEX2: A complete structure solution, refinement and analysis program. *J. Appl. Crystallogr.* **2009**, *42*, 339–341. [[CrossRef](#)]
50. Mos, A.; Castro, C.; Indris, S.; Ströbele, M.; Fink, R.F.; Meyer, H.-J. From WCl_6 to WCl_2 : Properties of Intermediate Fe–W–Cl Phases. *Inorg. Chem.* **2015**, *54*, 9826–9832. [[CrossRef](#)]
51. Ströbele, M.; Mos, A.; Meyer, H.-J. Cluster harvesting by successive reduction of a metal halide with a nonconventional reduction agent: A benefit for the exploration of metal-rich halide systems. *Inorg. Chem.* **2013**, *52*, 6951–6956. [[CrossRef](#)] [[PubMed](#)]
52. Ströbele, M.; Meyer, H.-J. Pandora’s box of binary tungsten iodides. *Dalton Trans.* **2019**, *48*, 1547–1561. [[CrossRef](#)]
53. Lizarazo-Jaimes, E.H.; Reis, P.G.; Bezerra, F.M.; Rodrigues, B.L.; Monte-Neto, R.L.; Melo, M.N.; Frezard, F.; Demicheli, C. Complexes of different nitrogen donor heterocyclic ligands with $SbCl_3$ and $PhSbCl_2$ as potential antileishmanial agents against Sb(III)-sensitive and -resistant parasites. *J. Inorg. Biochem.* **2014**, *132*, 30–36. [[CrossRef](#)]
54. Kalmutzki, M.; Ströbele, M.; Bettinger, H.F.; Meyer, H.-J. Development of Metal Cyanurates: The Example of Barium Cyanurate (BCY). *Eur. J. Inorg. Chem.* **2014**, *2014*, 2536–2543. [[CrossRef](#)]
55. Kalmutzki, M.; Ströbele, M.; Ensling, D.; Jüstel, T.; Meyer, H.-J. Synthesis, Structure, and Luminescence of Rare Earth Cyanurates. *Eur. J. Inorg. Chem.* **2015**, *2015*, 134–140. [[CrossRef](#)]
56. Salah, T.; Mhadhbi, N.; Ben Ahmed, A.; Hamdi, B.; Krayem, N.; Loukil, M.; Guesmi, A.; Khezami, L.; Houas, A.; Ben Hamadi, N. Physico-Chemical Characterization, DFT Modeling and Biological Activities of a New Zn(II) Complex Containing Melamine as a Template. *Crystals* **2023**, *13*, 746. [[CrossRef](#)]
57. Li, F.; Xu, H.; Xu, X.; Cang, H.; Xu, J.; Chen, S. Supramolecular salts assembled by melamine and two organic hydroxyl acids: Synthesis, structure, hydrogen bonds, and luminescent property. *CrystEngComm* **2021**, *23*, 2235–2248. [[CrossRef](#)]
58. Mitra, M.; Hossain, A.; Manna, P.; Choudhury, S.R.; Kaenket, S.; Helliwell, M.; Bauzá, A.; Frontera, A.; Mukhopadhyay, S. Melamine-mediated self-assembly of a Cu(II)–methylmalonate complex assisted by $\pi+\pi+$ and anti-electrostatic H-bonding interactions. *J. Coord. Chem.* **2017**, *70*, 463–474. [[CrossRef](#)]

59. Araar, H.; Benounis, M.; Direm, A.; Touati, A.; Atailia, S.; Barhoumi, H.; Jaffrezic-Renault, N. A new thin film modified glassy carbon electrode based on melaminium chloride pentachlorocuprate (II) for selective determination of nitrate in water. *Mon. Chem.* **2019**, *150*, 1737–1744. [[CrossRef](#)]
60. Hesse, M.; Meier, H.; Zeeh, B. *Spektroskopische Methoden in der Organischen Chemie*; Georg Thieme: Stuttgart, Germany, 2005.
61. Pavia, D.L.; Lampman, G.M.; Kriz, G.S.; Vyvyan, J.A. *Introduction to Spectroscopy*; Cengage Learning: Boston, MA, USA, 2014; pp. 14–101.
62. Lotsch, B.V.; Döblinger, M.; Sehnert, J.; Seyfarth, L.; Senker, J.; Oeckler, O.; Schnick, W. Unmasking melon by a complementary approach employing electron diffraction, solid-state NMR spectroscopy, and theoretical calculations—Structural characterization of a carbon nitride polymer. *Chem.-Eur. J.* **2007**, *13*, 4969–4980. [[CrossRef](#)]

Disclaimer/Publisher's Note: The statements, opinions and data contained in all publications are solely those of the individual author(s) and contributor(s) and not of MDPI and/or the editor(s). MDPI and/or the editor(s) disclaim responsibility for any injury to people or property resulting from any ideas, methods, instructions or products referred to in the content.